Electronic transport calculations for the conductance of Pt–1,4-phenylene diisocyanide–Pt molecular junctions

2010 Nanotechnology 21 155203

(http://iopscience.iop.org/0957-4484/21/15/155203)

Nanotechnology **21** (2010) 155203 (6pp) doi:10.1088/0957-4484/21/15/155203

Electronic transport calculations for the conductance of Pt–1,4-phenylene diisocyanide–Pt molecular junctions

Ruoxing Zhang[1,2], Guohui Ma[1], Meilin Bai[1], Lili Sun[1], Ivan Rungger[2], Ziyong Shen[1], Stefano Sanvito[2] and Shimin Hou[1,3]

[1] Key Laboratory for the Physics and Chemistry of Nanodevices, Department of Electronics, Peking University, Beijing 100871, People's Republic of China
[2] School of Physics and CRANN, Trinity College, Dublin 2, Republic of Ireland

E-mail: smhou@pku.edu.cn

Received 27 December 2009, in final form 8 February 2010
Published 23 March 2010
Online at stacks.iop.org/Nano/21/155203

Abstract

The low-bias transport properties of a single 1,4-phenylene diisocyanide (PDI) molecule connected to two platinum (Pt) electrodes are investigated using a self-consistent *ab initio* approach that combines the non-equilibrium Green's function formalism with density functional theory. Our calculations demonstrate that the zero-bias conductance of an asymmetric Pt–PDI–Pt junction, where the PDI molecule is attached to the atop site at one Pt(111) electrode and to a Pt adatom at the other, is $2.6 \times 10^{-2} G_0$, in good agreement with the experimental value ($3 \times 10^{-2} G_0$) measured with break junctions. Although the highest occupied and the lowest unoccupied molecule orbitals in PDI are both π-type, delocalized along the entire molecule, their electronic coupling with the highly conducting states of the Pt electrode is blocked at the atop site, leading to the small transmission. This indicates that more efficient electronic contacts are needed to fabricate molecular devices with a high conductance using Pt electrodes and aromatic isocyanides such as PDI.

(Some figures in this article are in colour only in the electronic version)

1. Introduction

In recent years electronic devices incorporating single molecules have received continuously growing attention, and molecular electronics is now believed to be one of the most promising solutions for tackling the limitations of silicon-based microelectronic device miniaturization [1, 2]. Besides gold, platinum is widely used as an electrode material for molecular devices, due to its high conductivity and chemical inertness [3–7]. In order to firmly connect individual molecules to the Pt electrodes, appropriate anchoring groups such as thiol, amine and isocyanide are typically employed. In particular, the isocyanide group has attracted widespread attention [8], since it is believed that the presence of a triple bond may effectively connect the p–π orbitals residing on the central aromatic moiety to the d–π orbitals pointing out of the Pt surface. Thus, a highly conductive transport channel is forecasted. However, the experimentally measured conductance of the 1,4-phenylene diisocyanide (PDI) anchored to Pt electrodes is only $3 \times 10^{-2} G_0$ [4], which is much less than the conductance, $1 G_0$, measured for the Pt–benzene–Pt junction [6] ($G_0 = 2e^2/h$ is the quantum conductance). Although preliminary theoretical studies on the electronic transport properties of the Pt–PDI–Pt junction have been reported [9, 10], the calculated value of the zero-bias junction conductance is almost one order of magnitude higher than that measured experimentally [9, 4]. Therefore, in order to elucidate the conducting mechanism of the Pt–PDI–Pt junction, more detailed studies on the relation between the electronic transport properties and the junction structure are highly desirable.

In this paper, we focus on the atomic structure and the low-bias transport properties of the Pt–PDI–Pt molecular junctions. This is investigated by using a fully self-consistent *ab initio* method that combines the non-equilibrium

[3] Author to whom any correspondence should be addressed.

Green's function (NEGF) formalism with density functional theory (DFT) [11–14], i.e., the so-called NEGF + DFT approach [15–20]. Our calculations demonstrate that the zero-bias conductance of an asymmetric Pt–PDI–Pt junction, where the PDI molecule is attached to the atop site of one Pt(111) electrode and to a Pt adatom of the other, is $2.6 \times 10^{-2} G_0$, consistent with the measured value [4]. Such a low transmission around the Fermi energy (E_F) is due to the inefficient electronic coupling of the highest occupied molecular orbital (HOMO) and the lowest unoccupied molecular orbital (LUMO) of PDI to the highly conducting states of the Pt electrodes. This occurs despite the fact that the PDI HOMO and LUMO are both π-type orbitals delocalized along the entire molecule.

2. Calculation method

We mainly use two computer programs for this work: the SIESTA code [21] to study the atomic structure of Pt–PDI–Pt junctions and the quantum transport code SMEAGOL [20, 22, 23] to study their electronic transport properties. SIESTA is an efficient DFT package, which adopts a finite range numerical orbital basis set to expand the wavefunctions of the valence electrons and makes use of improved Troullier–Martins pseudopotentials for the atomic cores [21, 24]. By means of extensive optimization, a user-defined double zeta plus polarization basis set is constructed for the carbon, nitrogen and hydrogen atoms, and a single zeta plus polarization basis set is used for Pt atoms. The Perdew–Burke–Ernzerhof (PBE) generalized gradient approximation (GGA) for the exchange and correlation functional is used in all our calculations to account for the electron–electron interactions [25]. Geometry optimization is performed by conjugate gradient relaxation until the forces are smaller than 0.03 eV Å^{-1}. For comparison, all-electron DFT calculations for the isolated PDI molecule are also carried out using both the PBE GGA functional and the Becke three-parameter Lee–Yang–Parr (B3LYP) semi-empirical hybrid functional with the Gaussian 03 code [26, 27]. Here, the 6-311++G(d, p) basis sets are used for C, H and N atoms [28].

SMEAGOL is a practical implementation of the NEGF + DFT approach, which uses SIESTA as the DFT platform [20, 22, 23]. We use an equivalent cutoff of 200.0 Ryd for the real space grid, while the charge density is integrated over 80 energy points along the semi-circle, 40 energy points along the line in the complex plane, 40 energy points along the real axis, and 20 poles are used for the Fermi function (the electronic temperature is 25 meV). We always consider periodic boundary conditions in the plane transverse to the transport. The unit cell of the extended molecule, for which the self-consistent calculation is performed, comprises one PDI molecule and ten Pt(111) atomic layers with a (3×3) supercell. The current–voltage (I–V) characteristics of the Pt–PDI–Pt molecular junctions can be calculated using

$$I = \frac{2e}{h} \int_{-\infty}^{+\infty} T(V, E)[f(E - \mu_L) - f(E - \mu_R)]\,\mathrm{d}E, \quad (1)$$

Table 1. Optimized bond lengths of the PDI molecule in the gas phase. The experimental values are also given for comparison.

		Gaussian 03		
Bond	SIESTA	PBE	B3LYP	Exp.[a]
N≡C	1.195	1.188	1.175	1.176
C_{ipso}–N	1.381	1.383	1.383	1.388
C_{ortho}–C_{ipso}	1.404	1.406	1.399	1.400
C_{ortho}–C_{meso}	1.391	1.392	1.387	1.400

[a] Reference [29].

where $T(V, E)$ is the transmission coefficient of the junction obtained at the applied bias V, $f(E)$ is the Fermi function, $\mu_{L/R} = E_F \pm eV/2$ is the local Fermi level of the left/right Pt electrode and E_F is the Fermi energy of the Pt bulk. The zero-bias junction conductance is related to the equilibrium transmission coefficient at the Fermi energy through the Landauer formula $G = \frac{2e^2}{h} T(V = 0, E_F)$. Then, the transmission coefficient $T(V, E)$ of the Pt–PDI–Pt molecular junctions is evaluated as

$$T(V, E) = \frac{1}{\Omega_{2DBZ}} \int_{2DBZ} T(\vec{k}; V, E)\,\mathrm{d}\vec{k}, \quad (2)$$

where Ω_{2DBZ} is the area of the two-dimensional Brillouin zone (2DBZ) in the transverse directions. The k-dependent transmission coefficient $T(\vec{k}; V, E)$ is obtained as

$$T(\vec{k}; V, E) = \mathrm{Tr}[\Gamma_L G_M^R \Gamma_R G_M^{R+}], \quad (3)$$

where G_M^R is the retarded Green's function matrix of the extended molecule and $\Gamma_{L(R)}$ is the broadening function matrix describing the interaction of the extended molecule with the left (right) electrode. More details on the method can be found in [20, 22, 23].

3. Results and discussion

First we investigate the atomic and electronic structure of PDI in the gas phase. Due to the presence of the two isocyano groups, the symmetry of PDI is only D_{2h} (see figure 1(a)), which is much lower than the symmetry D_{6h} of benzene. The optimized geometrical parameters of the PDI molecule are listed in table 1. As we can see, the N–C bond length of the isocyano group is calculated to be 1.195 Å by Siesta–PBE, i.e., it is about 0.02 Å larger than the corresponding experimental value extracted from electron diffraction [29]. Such a short bond length indicates that N–C is a triple bond. In contrast, the calculated bond length between the nitrogen atom in the isocyano group and the ipso carbon atom in the benzene backbone is underestimated by 0.007 Å. Although only an average value (1.400 Å) of the ring C–C bonds in the gas-phase PDI was determined by electron diffraction due to the limited resolution, the calculated difference (0.013 Å) between the C_{ipso}–C_{ortho} bond and the C_{ortho}–C_{meso} bond is comparable to the experimental value (0.011 Å) for a PDI single crystal as measured by the x-ray diffraction [29]. The same trend is also observed for the all-electron DFT calculation performed by using the same PBE GGA functional but with a much larger

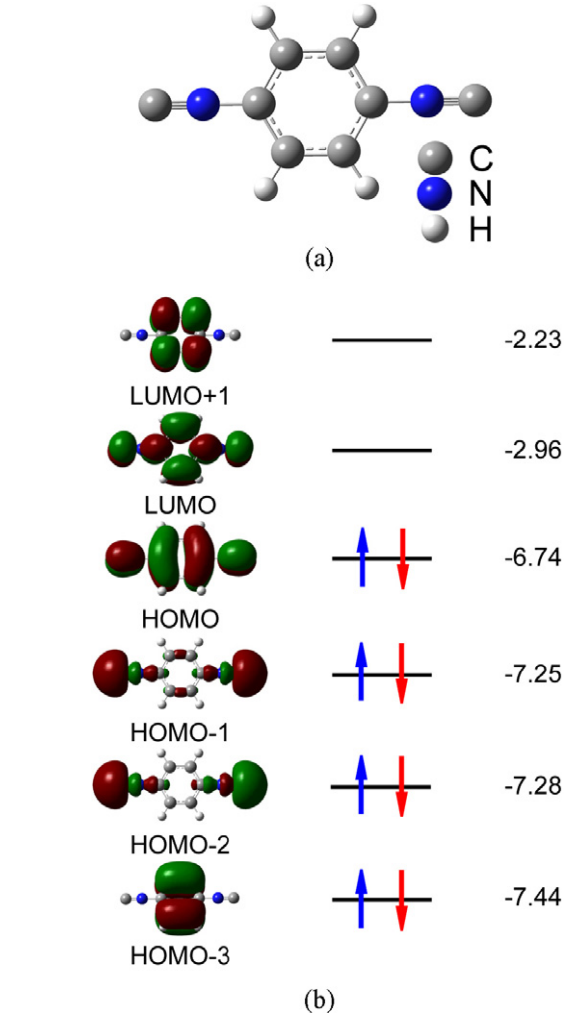

Figure 1. (a) Optimized molecular structure of the gas-phase PDI molecule, (b) energy diagram of frontier molecular orbitals in units of eV.

basis set (Gaussian 03). This confirms the appropriateness of the pseudopotentials and basis functions for the C, N and H atoms built for this work. Certainly the deviation from the experimental values of the bond lengths calculated with the B3LYP hybrid functional is smaller than that of the GGA, reflecting a well-known behavior of hybrid functionals for organic compounds [30].

Since the electronic transport properties of molecular junctions are strongly affected by the electronic interaction, the charge transfer and the energy level alignment at the molecule/electrode interfaces, it is interesting to take a look at frontier molecular orbitals of PDI (figure 1(b)). It is well known that both the HOMO and LUMO of benzene are doubly degenerate. In PDI, however, the degeneracy of the π-type orbitals of the benzene backbone is lifted by the two isocyano groups. For example, the doubly degenerate unoccupied π-type orbital splits into two components, the orbital component with a large density on the two ipso carbon atoms interacts constructively with the symmetric combination of the two π^* bonds of the isocyano groups, forming the delocalized PDI LUMO. The other orbital has no density on the two ipso carbon atoms and thus cannot be stabilized by interaction with the isocyano groups. This becomes the localized LUMO + 1. Similarly, the doubly degenerate occupied π-type orbital also splits into two components: the orbital component with two allylic-like fragments interacts destructively with the two π-bonds of the two isocyano groups if they are positive on one isocyano group and negative on the other, forming the PDI HOMO delocalized over the entire molecule; a second orbital has no density on the two ipso carbon atoms and becomes the localized HOMO-3. Therefore, the HOMO–LUMO gap of PDI, calculated to be 3.78 eV, is about 1.3 eV smaller than the benzene HOMO–LUMO gap (5.12 eV) calculated with the same PBE functional. In contrast to these π-type orbitals, the HOMO-1 and HOMO-2 are both σ-type and they are composed of the symmetric and antisymmetric combination of the two σ^* bonds of the two isocyano groups.

Now we move to investigate the low-bias transport properties of a single PDI molecule sandwiched between Pt electrodes. Since experimental evidence from surface-enhanced Raman spectroscopy measurements seems to indicate that PDI molecules bind to the Pt(111) surface with a terminal geometry [31], we first study the case of PDI vertically placed on the atop sites of the two Pt electrodes (see figure 2(a)). After optimization, the lengths of the Pt–C bond and the N–C bond in the isocyano group and the N–C_{ipso} bond are determined to be respectively 1.872 Å, 1.186 Å and 1.369 Å. When compared to those of PDI in the gas phase, both the N–C bond in the isocyano group and the N–C_{ipso} bond are slightly shortened. The corresponding zero-bias transmission coefficient $T(E)$ is given in figure 2(b), together with the transmission projected onto the PDI HOMO and LUMO obtained by using our previously developed scattering states projection method [32]. As we can see, although the HOMO and LUMO are both π-type orbitals delocalized over the entire molecule, their transmission peaks are respectively centered at around 2.4 eV below and 1.3 eV above E_F. Therefore, $T(E_F)$ is only 0.6×10^{-2}, indicating that tunneling is the dominant conduction mechanism for PDI symmetrically connected to Pt at the atop site. This is corroborated by the calculated I–V curve (figure 2(c)), which is basically linear in the low-bias range.

In order to get a better insight into the interaction between PDI and the Pt electrodes when the anchoring is at the atop site, figure 2(d) provides the density of states (DOS) of the junction projected onto the frontier molecular orbitals of PDI. Similarly to the adsorption of carbon monoxide (CO) on Pt(111) surfaces [33], charge transfer also occurs in the Pt–PDI–Pt junction. Here, electron donation from the PDI molecule to the Pt electrodes mainly originates from the HOMO-1 and HOMO-2, whose broadened DOS extends above E_F due to their strong interaction with the Pt atoms at the atop site of the (111) surface. In contrast, the HOMO only makes a negligible contribution to the electron transfer, though it is closer to E_F than the HOMO-1 and HOMO-2 orbitals. Similarly, only a small tail of the broadened DOS of the LUMO extends below the Fermi energy, thus the electron transfer from the Pt electrodes to the PDI molecule is relatively small. Therefore, in the Pt–PDI–Pt junction contacted symmetrically

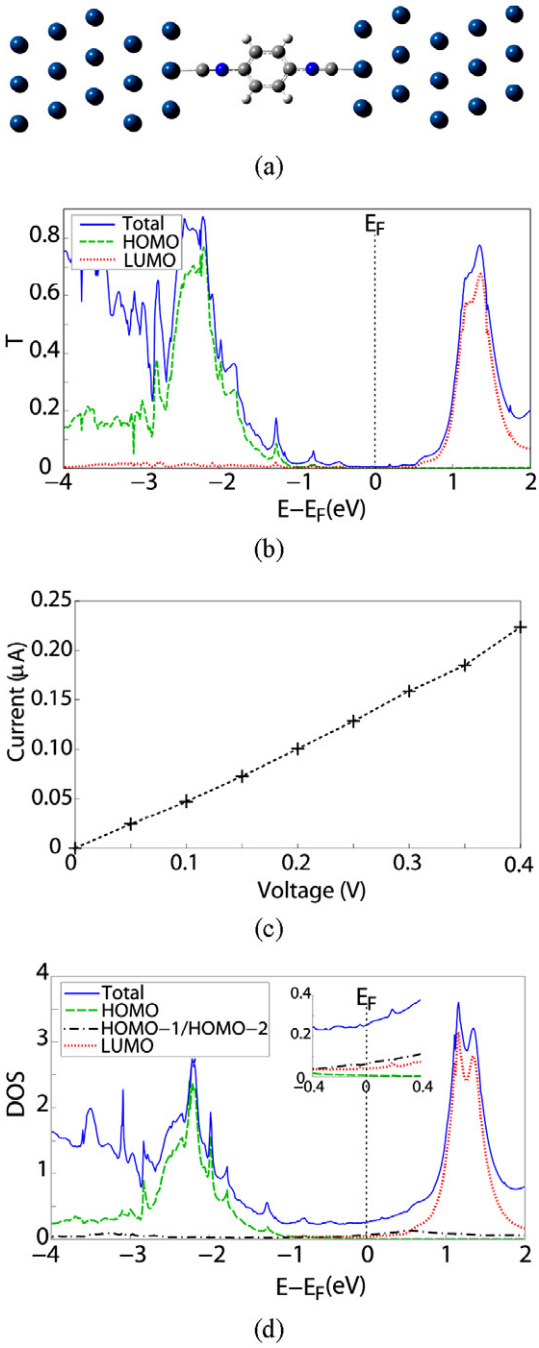

Figure 2. Transport properties of a PDI molecule attached symmetrically to two Pt electrodes at the atop site: (a) optimized geometry; (b) energy-dependent transmission function together with the projected transmission onto the PDI HOMO and LUMO; (c) the I–V curve; (d) DOS projected onto the PDI frontier molecular orbitals, the inset is an enlarged figure around the Fermi energy.

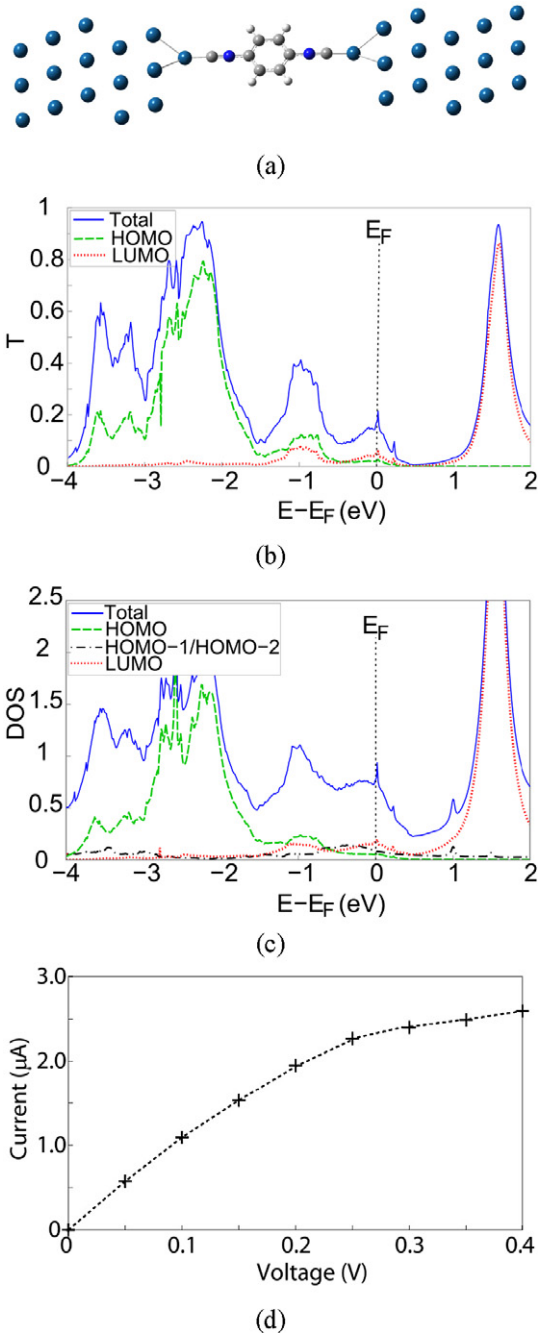

Figure 3. Transport properties for a PDI molecule attached symmetrically to two Pt electrodes through a Pt adatom: (a) optimized geometry; (b) energy-dependent transmission function together with the projected transmission onto the PDI HOMO and LUMO; (c) DOS projected onto the PDI frontier molecular orbitals; (d) the I–V curve.

at the atop sites, the junction conductance is very small though the interactions of N with C in the isocyano group and those in the benzene backbone at the ipso position are both strong.

In the scanning tunneling microscope (STM) break junction method [4], Pt quantum point contacts are usually produced before the formation of Pt–PDI–Pt junctions, indicating that atomic protrusion will exist on the surface of the Pt electrodes [34, 35]. In order to simulate this situation we investigate next the transport properties of a PDI molecule sandwiched symmetrically between two Pt(111) electrodes through one Pt adatom on each side (see figure 3(a)). The lengths of the Pt–C bond and the N–C bond in the isocyano group and the N–C_{ipso} bond are optimized to be about 1.898 Å, 1.202 Å and 1.379 Å, respectively. At variance with the junction contacted at the atop sites, here the N–C bond in the isocyano group is slightly longer than that of PDI in the gas phase, although the N–C_{ipso} bond is still a little shorter.

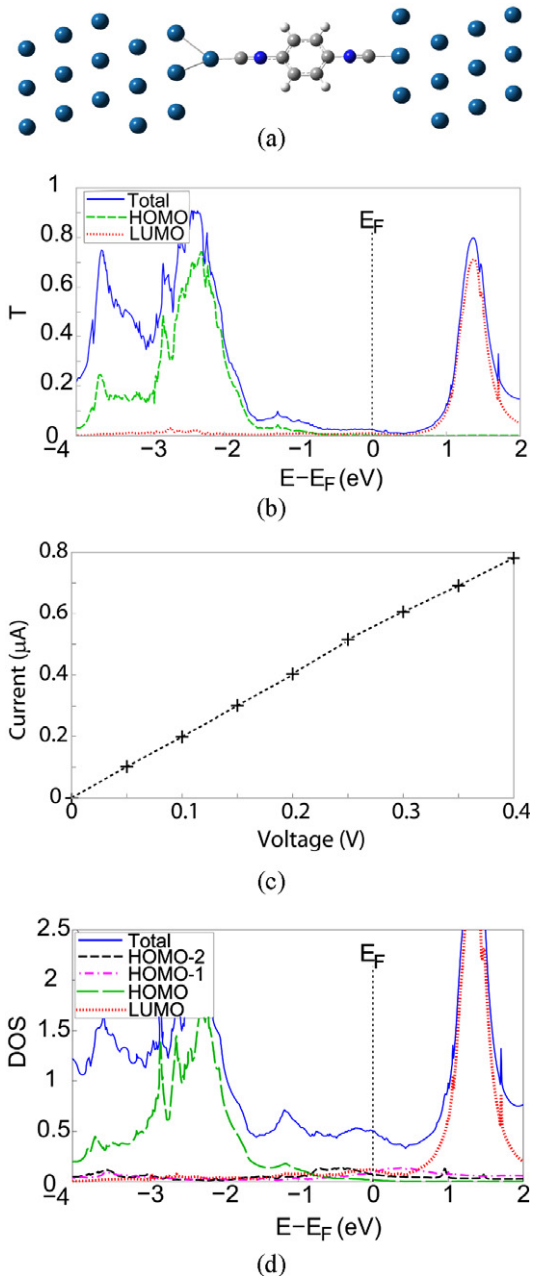

Figure 4. Transport properties for a PDI molecule attached asymmetrically to Pt electrodes at the atop site on one side and to a Pt adatom on the other side: (a) optimized geometry; (b) energy-dependent transmission function together with the projected transmission onto the PDI HOMO and LUMO; (c) the I–V curve; (d) DOS projected onto the PDI frontier molecular orbitals.

In figure 3(b) we present the calculated zero-bias transmission coefficient and the contributions made by the PDI HOMO and LUMO. When compared to the junction contacted at the atop sites, we find that the most striking difference is the significant enhancement of the transmission around E_F, with $T(E_F) = 0.17$. The HOMO and LUMO now contribute not only to the transmission peaks located respectively at 2.4 eV below and 1.6 eV above the Fermi energy, but also to the small transmission peak at around E_F and to that centered at around 1.0 eV below E_F. This result is corroborated by the DOS projected onto the frontier molecular orbitals of PDI, shown in figure 3(c). As we can see, both the HOMO electron donation and the LUMO electron subtraction are enhanced, since the portions of the HOMO and LUMO broadened DOS crossing the Fermi energy are both increased. In this case the HOMO and LUMO of PDI are both π-type orbitals delocalized over the entire molecule, therefore they can form more efficient conducting channels than the localized σ-type HOMO-1 and HOMO-2, leading to a higher transmission around E_F. Thus, as shown in figure 3(d), a much larger current can be conducted through the PDI molecule when it is connected to the Pt electrodes through two Pt adatoms.

Finally, we study the transport properties of a PDI molecule sandwiched between two Pt electrodes with an asymmetric bonding geometry. That is, PDI is connected to the Pt(111) electrodes at the atop site at one side and at a Pt adatom at the other (see figure 4(a)). The zero-bias transmission coefficient at the Fermi energy for this asymmetric junction is calculated to be 2.6×10^{-2}, which compares rather well with the experimentally measured value of 3×10^{-2} [4]. This better agreement should not be surprising. In fact, in STM break junction experiments [4] a Pt thin film composed of grains with an atomically flat (111) surface is used as the bottom electrode and an extremely sharp Pt STM tip makes electrical contact. Thus, a PDI molecule is likely to chemically adsorb at the atop site of the Pt(111) surface through one isocyano group, and to be bonded to an undercoordinated Pt site at the STM tip through the other isocyano group. In support to this picture, the binding energies of PDI on the Pt(111) surface at the atop and adatom sites are calculated to be respectively 2.21 eV and 2.32 eV.

The overall shape of both the zero-bias transmission curve around E_F and the I–V curve of the asymmetric Pt–PDI–Pt junction (figures 4(b) and (c)) is similar to that of the junction symmetrically contacted at the atop sites, further demonstrating that the atop bonding geometry provides a weak electronic contact for PDI on Pt. Although in the asymmetric Pt–PDI–Pt junction the DOS of the PDI LUMO still extends below E_F, due to the presence of a Pt adatom on the surface of one of the electrodes (see figure 4(d)), still the LUMO cannot provide a good conducting channel since its electronic coupling with the highly conducting Pt states is blocked by the atop site at the other electrode. Therefore, the atop site dominates the low-bias conductance of the asymmetric Pt–PDI–Pt junction.

4. Conclusion

In this work we have investigated the electronic structure and transport properties of PDI molecules sandwiched between Pt electrodes. Due to the presence of the two isocyano groups, the electronic structure of PDI is drastically different from that of benzene. Although the PDI HOMO-3, HOMO, LUMO and LUMO + 1 are all π-type orbitals, the HOMO and LUMO are delocalized along the entire molecule while the HOMO-3 and LUMO + 1 are localized over the benzene backbone. Furthermore, the HOMO-1 and HOMO-2 are both σ-type orbitals localized over the two isocyano groups. Therefore, the electronic coupling of the HOMO and LUMO of PDI with the

Pt electrodes determines the low-bias transport properties of the Pt–PDI–Pt junctions.

In the symmetric Pt–PDI–Pt junction contacted at the atop sites the HOMO-1 and HOMO-2 orbitals are responsible for the electron transfer, but both the HOMO and the LUMO remain far from the Fermi energy, thus $T(E_F)$ is dominated by tunneling. By changing the bonding geometry from the atop sites to Pt adatoms, one significantly enhances the coupling of the PDI HOMO and LUMO with the highly conducting states of the Pt electrodes, thus $T(E_F)$ is greatly increased. However, none of these two geometrical configurations reproduce the STM break junction experiments well, since the one with atop site bonding is too insulating while that with adatoms is too conductive. The situation is drastically improved when one considers asymmetric junctions, where the anchoring to the electrodes is through a Pt adatom on one side and the atop position on the other. In this case we find $T(E_F) = 2.6 \times 10^{-2}$, in excellent agreement with experiments. Our results are thus consistent with the expectation that in STM break junctions PDI will chemically bind at the atop site on the Pt(111) substrate and to an adatom at the STM tip.

Further studies on how to improve the electronic coupling of π-type delocalized orbitals with the electrodes' conducting channels, so that highly conductive devices can be made, will be pursued in the future.

Acknowledgments

This project was supported by the National Natural Science Foundation of China (nos 60771002 and 60971002), the Ministry of Education (NCET-07-0014), the MOST of China (nos 2006CB932404 and 2007CB936204) and the CSC program of China. The Smeagol Project (SS) is sponsored by the Science Foundation of Ireland.

References

[1] Nitzan A and Ratner M A 2003 *Science* **300** 1384
[2] Tao N J 2006 *Nat. Nanotechnol.* **1** 173
[3] Djukic D, Thygesen K S, Untiedt C, Smit R H M, Jacobsen K W and van Ruitenbeek J M 2005 *Phys. Rev.* B **71** 161402(R)
[4] Kiguchi M, Miura S, Hara K, Sawamura M and Murakoshi K 2007 *Appl. Phys. Lett.* **91** 053110
[5] Kiguchi M, Miura S, Takhashi T, Hara K, Sawamura M and Murakoshi K 2008 *J. Phys. Chem.* C **112** 13349
[6] Kiguchi M, Tal O, Wohlthat S, Pauly F, Krieger M, Djukic D, Cuevas J C and van Ruitenbeek J M 2008 *Phys. Rev. Lett.* **101** 046801
[7] Kiguchi M 2009 *Appl. Phys. Lett.* **95** 073301
[8] Angelici R J and Lazar M 2008 *Inorg. Chem.* **47** 9155
[9] Seminario J M, De La Cruz C E and Derosa P A 2001 *J. Am. Chem. Soc.* **123** 5616
[10] Morari C, Rignanese G-M and Melinte S 2007 *Phys. Rev.* B **76** 115428
[11] Meir Y and Wingreen N S 1992 *Phys. Rev. Lett.* **68** 2512
[12] Thygesen K S 2006 *Phys. Rev.* B **73** 035309
[13] Hohenberg P and Kohn W 1964 *Phys. Rev.* **136** B864
[14] Kohn W and Sham L J 1965 *Phys. Rev.* **140** A1133
[15] Zhang J, Hou S, Li R, Qian Z, Han R, Shen Z, Zhao X and Xue Z 2005 *Nanotechnology* **16** 3057
[16] Xue Y, Datta S and Ratner M A 2002 *Chem. Phys.* **281** 151
[17] Ke S-H, Baranger H U and Yang W 2004 *Phys. Rev.* B **70** 085410
[18] Taylor J, Guo H and Wang J 2001 *Phys. Rev.* B **63** 245407
[19] Brandbyge M, Mozos J-L, Ordejón P, Taylor J and Stokbro K 2002 *Phys. Rev.* B **65** 165401
[20] Rocha A R, García-Suárez V M, Bailey S, Lambert C, Ferrer J and Sanvito S 2006 *Phys. Rev.* B **73** 085414
[21] Soler J M, Artacho E, Gale J D, García A, Junquera J, Ordejón P and Sánchez-Portal D 2002 *J. Phys.: Condens. Matter* **14** 2745
[22] Rocha A R, García-Suárez V M, Bailey S, Lambert C, Ferrer J and Sanvito S 2005 *Nat. Mater.* **4** 335
[23] Rungger I and Sanvito S 2008 *Phys. Rev.* B **78** 035407
[24] Troullier N and Martins J 1991 *Phys. Rev.* B **43** 1993
[25] Perdew J, Burke K and Ernzerhof M 1996 *Phys. Rev. Lett.* **77** 3865
[26] Stephens P J, Devlin F J, Chabalowski C F and Frisch M J 1994 *J. Phys. Chem.* **98** 11623
[27] Frisch M J *et al* 2003 *Gaussian 03, Revision C02* (Pittsburg, PA: Gaussian Inc.)
[28] Frisch M J, Pople J A and Binkley J S 1984 *J. Chem. Phys.* **80** 3265
[29] Colapietro M, Domenicano A, Portalone G, Torrinin I, Hargittai I and Schultz G 1984 *J. Mol. Struct.* **125** 19
[30] Koch W and Holthausen M C 2001 *A Chemist's Guide to Density Functional Theory* 2nd edn (Weinheim: Wiley–VCH)
[31] Gruenbaum S M, Henney M H, Kumar S and Zou S 2006 *J. Phys. Chem.* B **110** 4782
[32] Li R, Hou S, Zhang J, Qian Z, Shen Z and Zhao X 2006 *J. Chem. Phys.* **125** 194113
[33] Stroppa A, Termentzidis K, Paier J, Kresse G and Hafner J 2007 *Phys. Rev.* B **76** 195440
[34] Bahn S R and Jacobsen K W 2001 *Phys. Rev. Lett.* **87** 266101
[35] Garcia-Suarez V M, Rocha A R, Bailey S W, Lambert C J, Sanvito S and Ferrer J 2005 *Phys. Rev. Lett.* **95** 256804